Pergamon

Cement and Concrete Research, Vol. 25, No. 3, pp. 522-530, 1995

0008-8846/95 $9.50+.00

0008-8846(95)00041-0

NUMERICAL SIMULATION OF HYDRATION AND MICROSTRUCTURAL DEVELOPMENT IN HARDENING CEMENT-BASED MATERIALS (II) Applications

K. van Breugel
Technical University of Technology
Delft, The Netherlands

(Refereed)
(Received July 28, 1992; in final form November 7, 1994)

ABSTRACT

After having outlined the structure of a computer-based simulation program, called HYMOSTRUC (9), which was developed to describe and predict hydration and microstructural development of cement-based materials, characteristic features of the simulation model are discussed. Attention is paid to changes in the number of particles in the early stage of hydration, the development of interparticle contacts and how this affects the rate of hydration and the effect of particle size on hydration characteristics. The correlation between strength and the amount of embedded cement, i.e., cement involved in the formation of interparticle contacts, and the influence of the w/c ratio and the curing temperature on this correlation is discussed. Calculated porosity in the matrix-aggregate interfacial zone is shown and compared with experimental results. The potential of the model to describe and predict isothermal and adiabatic hydration curves is illustrated with some examples and the accuracy of the results is discussed.

Introduction

With the simulation program HYMOSTRUC, hydration curves of Portland cement-based systems are calculated as a function of the chemical composition and particle size distribution of the cement, the w/c ratio and the reaction temperature. Microstructural development, i.e. the formation of interparticle contacts, is quantified explicitly as well as its effect on the rate of hydration. The allowance for microstructural development distinguishes the model from earlier proposed models. It is addressed in more detail in this paper.

Potential Of The Model To Explain And Describe Microstructural Aspects

Clustering of particles. Reduction of the number of free particles

As hydration proceeds small particles will become embedded in the outer shell of larger particle. Consequently the number of small *free particles* or *free clusters*, i.e. particles and clusters of par-

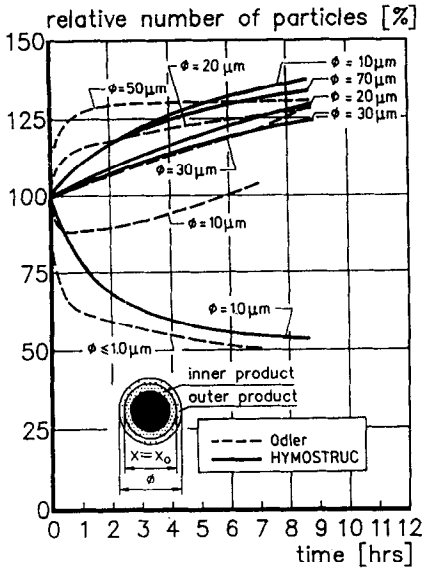

FIG. 1
Proportional changes in particle size distribution in a hydrating paste. Experimental (1) and theoretical (2).

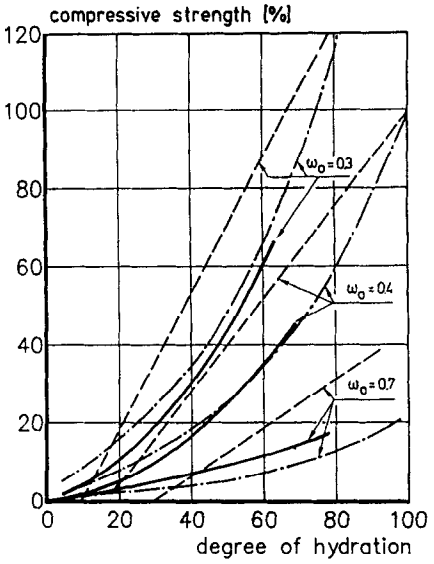

FIG. 2
Proportional increase in strength (Dashed: Fagerlund. Dash-dot: Powers) and of the volume of embedded cement v_{em}^{pa} (solid) (2).

ticles which are not embedded in the outer shell of larger particles decreases. Consequently the number of large particles or large clusters increases. This shift from a large number of small particles to a smaller number of large particles has been observed by Odler et al. (1). Results for an ordinary Portland cement paste, with $\omega_0 = 0.3$ and Blaine surface area = 300 m^2/kg, are presented in Fig. 1 by the dashed curves. The solid curves in the figure show the same phenomenon as it is quantified by HYMOSTRUC, although for a paste with w/c ratio $\omega_0 = 0.5$. A comparison of results is nevertheless judged warranted as in the early stage of hardening the influence of the w/c ratio is not significant as far as its effect on changes in the particle size distribution is concerned. Taking into account the experimental difficulties and experimental error when counting the number of particles in a hydrating mass and the simplifications embodied in HYMOSTRUC, it can be concluded that the experimental and theoretical data are in good agreement with each other. This warrants the conclusion that the concept of embedding small particles in the outer shell of larger ones as considered and modelled in HYMOSTRUC is not in contradiction with experimental results.

Embedded cement volume and strength development

The embedded cement volume, i.e. the amount of cement involved in interparticle interactions, is expected to be a possible strength parameter. In order to check the reasonableness of this assumption the proportional increase in the amount of embedded cement is compared with the proportional increase in strength calculated according to procedures proposed by Powers (10) and Fagerlund (11). These proportional increases are shown in Fig. 2 as a function of the degree of hydration for pastes with w/c ratios $\omega_0 = 0.3$, 0.4 and 0.7. The observed relatively good agreement between the three sets of curves suggest, as expected, a good correlation between strength and the amount of embedded cement.

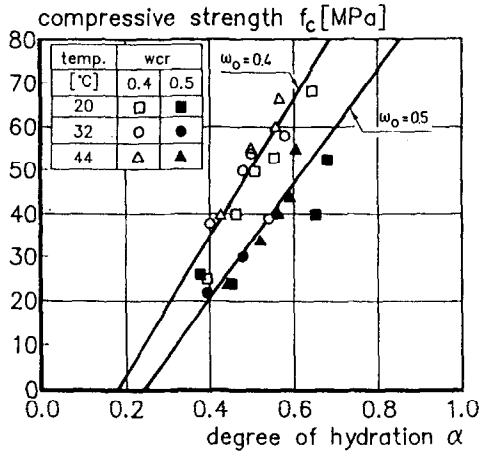

a. Strength vs. degree of hydration

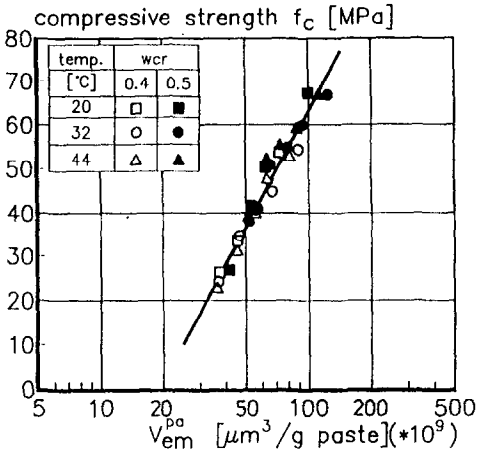

b. Strength vs. embedded cement volume

FIG. 3

Strength of cement mortar as a function of the degree of hydration (3a) and the amount of embedded cement v_{em}^{pa} [2]. (3b) (ref. (2)).

For pastes with w/c ratios $\omega_0 = 0.4$ and $\omega_0 = 0.5$ (Fig. 3), *absolute* values of the measured compressive strength are presented as a function of the calculated degree of hydration and the calculated amount of embedded cement per μm^3 paste. Whereas the relationship between strength and degree of hydration still exhibits a pronounced dependence on the w/c ratio (Fig. 3a), the relationship between strength and embedded cement volume is almost independent of the w/c ratio (Fig. 3b). This information tends to confirm the assumption that strength is correlated with the number of interparticle contacts, since the amount of embedded cement is probably a measure for the number of interparticle contacts.

The reasonableness of the assumed correlation between strength and embedded cement volume receives further support from an evaluation of the effect of the curing temperature on strength development. As discussed in Part I (9) higher temperatures would cause a reduction of the v-factor, i.e., the ratio of the gel to reactant volume. A smaller v-factor at elevated tempera-

TABLE 1.

Effect of curing temperature on compressive strength of pastes and embedded cement volume after 28 days hydration (2). Measurements by Rakel (21).

Curing temp.	Degree of hydration	Compressive strength at 28 d. (measured)		Embedded cement volume $v_{em,28}$ at $\alpha_{t=28}$ (calculated)	
T [°C]	(measured) $\alpha_{t=28}$	$f_{c,28}(T)$ [MPa]	$f_{c,28}(T)/f_{c,28}(22°C)$ relative	$v_{em,28}(T)$ [μm^3/g cement] x 10^9	$v_{em,28}(T)/v_{em,28}(22°)$ relative
22	0.730	60.8	100%	145	100%
30	0.734	53.4	88%	142	98%
40	0.734	51.3	84%	134	92%
50	0.754	48.5	80%	123	85%

tures causes less expansion of hydrating particles and hence a reduction in the amount of embedded cement, of the number of the interparticle contacts and, consequently, of the strength. The data presented in Table 1 seems to confirm the foregoing reasoning. The 28-days strengths of pastes, $f_{c,28}(T)$, cured at T = 22, 30, 40 and 50°C, respectively, is presented together with the calculated amount of embedded cement $v_{em,28}(T)$. The decrease in strength with increasing temperatures turns out to correlate quite well with the decrease in the amount of embedded cement. Thus there is good justification for considering the amount of embedded cement as a strength parameter which can explain strength development on a microstructural basis.

Predicted strength reductions of about 20% are also in good agreement with experimental data presented by Kjellsen et al. (22). Experimental work of Kjellsen et al. (22) shows strength reductions of 20....25% when the curing temperature is increased from 5°C to 50°C. With HYMOSTRUC a reduction of the amount of embedded cement of 22...28% is predicted (24), which reduction corresponds fairly well with the strength reductions found by Kjellsen.

Matrix-aggregate interfacial zone

Since HYMOSTRUC accounts for the stereological aspect of microstructural development explicitly, evaluation of the effect of the *packing of particles* in the interfacial zone on the porosity of the paste in this zone is possible. For a cement of moderate fineness Fig. 4 shows measured and calculated thickness and porosity of this zone. In order to enable comparison of the measured and calculated porosity, the porosity is presented in a dimensionless form. After 1 day of hydration the measured and calculated interfacial porosity are in good agreement with each other. At later ages the measured porosity is much less than the calculated porosity, particularly in the close vicinity of the aggregate surface. This discrepancy can be ascribed to the fact that in the calculated porosity only stereological-oriented effects are considered. In an actual paste, however, not only stereological aspects, but also chemistry-related aspects, i.e. densification of the matrix due to precipitation of calcium hydroxide in the water-rich interfacial zone, affect the porosity here. The latter effect is not considered explicitly in the present model.

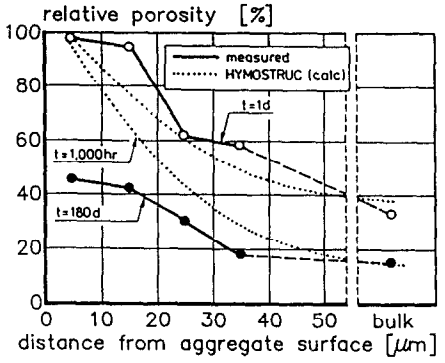

FIG. 4
Porosity in the matrix-aggregate interfacial zone.
Experimental data: Scrivener (5).

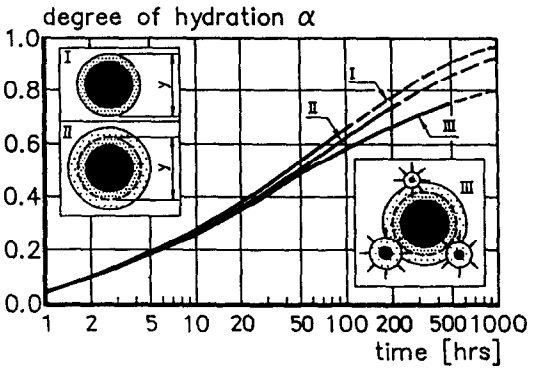

FIG. 5
Effect of extra particle expansion and water withdrawal mechanism on overall rate of hydration (2).

Factors Affecting The Rate Of Hydration

Effect of particle interaction on the overall rate of hydration

The effect of embedding small particles in the outer shell of larger particles is two-fold. First, embedding of particles causes an extra expansion of the large central particles, which will result in an extra diffusional resistance of the product layer. Second, embedded but still hydrating particles will withdraw water from the central particle in the outer shell of which they are embedded. The effects of these two aspects are illustrated in Fig. 5. For a cement paste with $\omega_0 = 0.4$, made of a cement with intermediate fineness, three simulations were conducted. In the first simulation, represented by curve I, no extra expansion caused by embedding of particles and water withdrawal was considered. Curve II refers to a simulation in which extra expansion due to embedding of particles was taken into account, whereas curve III reflects the effect of both extra particle expansion and water withdrawal. In order to clearly illustrate the effect of the two rate reducing factors the simulations have been carried out with arbitrary values of the basic rate factor $K_0(C_3S)$ and have been extended beyond a practical ultimate degree of hydration of about 0.7. For this value of the degree of hydration ignorance of extra particle expansion and water withdrawal reveals to cause a difference in the calculated degree of hydration of about 15%. Although this difference is a *model-bound* value and can, therefore, only give an *indication* of the effect of particle interaction on the rate of hydration, ignorance of the effect of particle interaction will almost inevitably lead to misinterpretations of test results with regard to hydration mechanisms and the values of rate constants and diffusion coefficients.

Rate of penetration of the reaction front

Initial rate of penetration

The initial rate of penetration of the reaction front is given by the basic rate factor $K_0(C_3S)$ [μm/h] and is, at first, the same for all particle diameters. For a large number of cements the $K_0(C_3S)$-values were found to range from 0.02 μm/h for a *low C_3S - high C_2S* cement to 0.07 μm/h for a *high C_3S - low C_2S* cement. These values have been compared with literature data in Table 2. Caution must be exercised when comparing these values, since most of them have been obtained by calculating back using the overall degree of hydration and the specific surface of the

TABLE 2
Rate of penetration of the reaction front in cement particles and compounds (2).
(Isothermal curing at 20°C)

Author	Ref.	year	reference period	material	penetration rate μm/h
Anderegg et al.	[12]	1929	0 - 24 h	cement	0.02
Krogbeumker	[13]	1972	0 - 72 h	Portland cement	0.032
Steinherz	[14]	1960	0 - 72 h	cement clinker	0.021
Tsumura	[15]	1966	first hrs	alite	0.055
				C_3S	0.036
				C_2S	0.0011
Lhopitallier et al.	[16]	1948	1st month	cement clinker	0.042
Taplin	[17]	1968	>1000 h	alite	0.0125
				β-C_2S	0.0009
Bezjak	[18]	1980	phase-bound	alite	0.067
			phase-bound	commercial cement	0.074-0.110

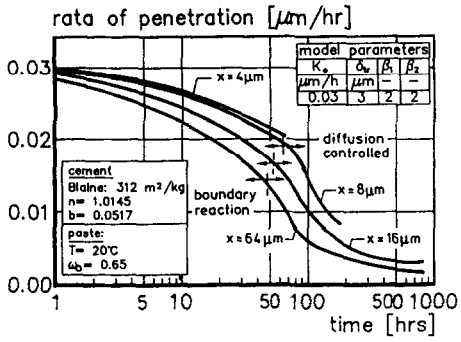

FIG. 6
Rate of penetration of the reaction front as a function of time (2).

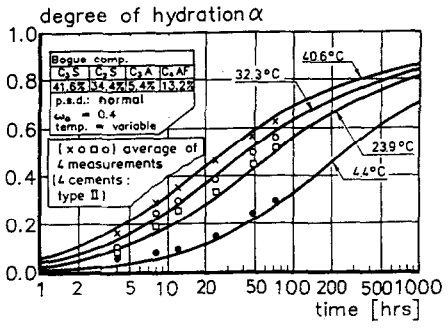

FIG. 7
Effect of (isothermal) temperature on degree of hydration. Experimental: discrete points (4). Calculated: solid lines (2).

cement. The latter quantity is strongly affected by assumptions concerning the shape of the cement particles and the measuring method, which results in a large scatter of data. Even bearing this in mind, one can conclude that the results are in good agreement with the data presented.

Evolution of the rate of penetration

As hydration proceeds, the rate of penetration will decrease due to the effect of different reduction mechanisms (2,9) For a paste with $\omega_0 = 0.65$ the rate of penetration of particles having size x = 4, 8, 16 and 64 μm is shown in Fig. 6. Because of the embedding of small particles, the expansion of larger particles exceeds that of small particles, so that larger ones will reach the diffusion controlled stage sooner than smaller ones. Moreover, the water withdrawal mechanism will affect the rate of penetration of the larger particles more than the small particles. Consequently, the rate of penetration at an arbitrary point of time will differ for different particle sizes. For low w/c ratios the rate of penetration of larger particles may tend to zero while at the same time smaller particles may still continue to hydrate.

Describing And Predicting The Degree Of Hydration

Effect of temperature and w/c ratio

The potential of HYMOSTRUC to simulate the effects of the curing temperature and the w/c ratio on the rate of hydration is illustrated in figures 7 and 8. The experiments are isothermal tests at four different temperatures carried out by Lerch at al. (4) and, again isothermal, tests on pastes with w/c ratios 0.25, 0.3, 0.4 and 0.5 carried out by Danielsson (7), respectively. Test data are given in the insets of the figures. Measured hydration values are indicated with discrete points, whereas the calculated hydration values are given by the solid lines.

Predictive potential of HYMOSTRUC

The figures 7 and 8 illustrate the potential of HYMOSTRUC to describe the hydration process for different temperatures and w/c ratios, respectively. Real predictions of hydration curves, i.e., simulations with the *default values* for the model parameters $K_0(C_3S)$, $\delta_{tr}(C_2S)$, β_1 and β_2 as defined in (9), are shown in the figures 9 and 10. In Fig. 9 two adiabatic temperature curves are presented for mixes with $\omega_0 = 0.4$ and $\omega_0 = 0.5$, respectively. The calculated curves are indicated

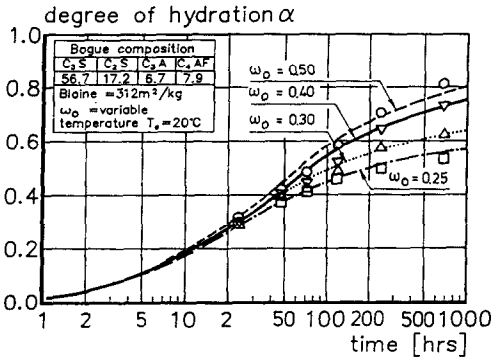

FIG. 8
Effect of w/c ratio on degree of hydration. Experimental: discrete points (7). Calculated: solid lines (2).

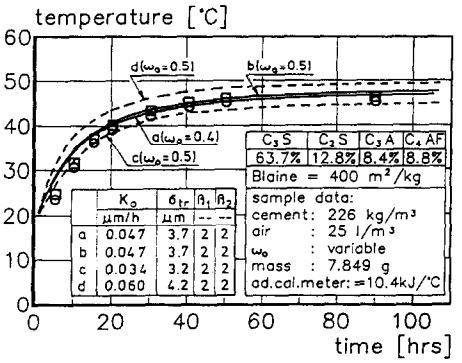

FIG. 9
Measured (discrete points) and predicted (solid and dashed lines) adiabatic hydration curves (2).

by the solid lines. For the mix with $\omega_0 = 0.5$ dashed lines indicate the predictions with 5% upper and lower bound values of $K_0(C_3S)$ and values for the transition thickness $\delta_{tr}(C_2S)$ 0.5 μm lower and higher than its default values (curves d and c). It can be concluded that the measured adiabatic temperature curves fall within the range bordered by the dashed curves calculated with the upper and lower bound values of the model parameters. In Fig. 10, taken from (23), predicted adiabatic hydration curves are compared with the results of a Round Robin test. In this test seven laboratories in different European countries participated. The Portland cement, sand and aggregate were provided by one of the participating laboratories. Tests were carried out with mixes with $\omega_0 = 0.6$. Cement, sand and aggregate wore mixed in proportion 1:2.5:3.5. The calculated clinker composition (Bogue) was: C_3S = 535 and C_2S = 16%. Specific surface (Blaine) = 372 m^2/kg.

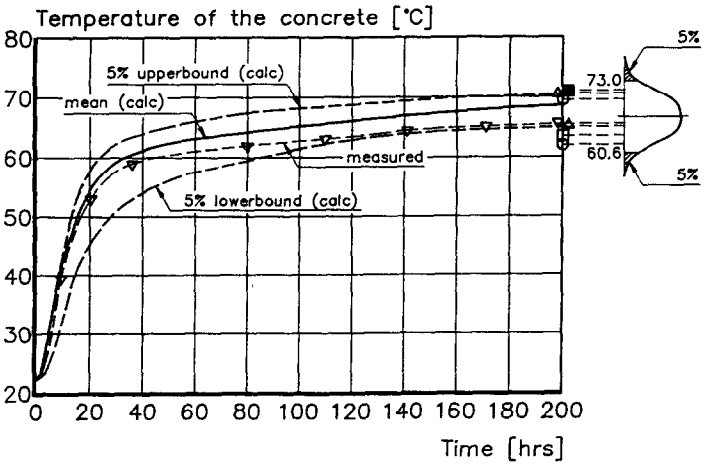

Fig. 10
Adiabatic test data obtained in a Round Robin tests compared with adiabatic curves predicted with HYMOSTRUC (24).
(Round Robin test conducted in framework of RILEM-TC/119)

In Fig. 10 four adiabatic curves are shown. The solid curve represents the calculated mean value of the adiabatic curve, whereas the dashed lines represent the predicted 5% upper and 5% lower bound values. The dashed line with the triangles shows an adiabatic curve measured in one of the participating laboratories. The mean value of value of the measured temperature rise after 200 hrs was 66.8°C with a multi-laboratory standard deviation 3.8°C. Assuming a normal distribution of the test results the 5% upper and lower bound temperatures at 200 hrs are 73.0 and 60.6°C, respectively. The 5% upper and lower bound temperatures predicted with HYMOSTRUC were 70.5° and 65.5°C, which corresponds quite good with the experimentally obtained values.

Discussion

When discussing microstructural characteristics of hardened cement-based materials Wittmann (3) stated in 1980 that, because of the actual complexity of the microstructure, there is no hope that we will ever be capable of modelling the microstructure of hardened cement realistically. If this statement holds for *hardened* cement paste, it certainly holds for *hardening* pastes. Six year later Diamond (6), discussing the work of Jennings on microstructural development in a C_3S paste, concluded in a similar way when stating: "While the concept (of Jennings) and some of the specifics of such modelling of microstructural development can be extended to Portland cement paste, such extension is extremely difficult because of the much greater complexity of the cement system, and success should not be expected in the near future". Against the background of these statements it is obvious that the simulation model discussed in these articles, viz. HYMOSTRUC, can not be more than an attempt, a step in a certain direction. On the other hand the author is convinced of the vast potential of computer-based simulations of complex, interrelated processes and mechanisms. The modern generation of computers enable us to make huge files of information operational from such fields as chemistry, physics, stereology and thermodynamics. Thus gaps are bridged between different disciplines involved and even between micro- and meso-levels on the one hand and the macro- or engineering levels on the other.

The step-wise calculation procedure according to which HYMOSTRUC operates makes it possible to consider non-linear phenomena and mechanisms which we would have to renounce if we would restrict ourself to a purely analytical "closed solution" approach. The open structure of the model makes it most flexible and therefore also most attractive for both research and practical applications.

An evaluation of the results of numerical simulations conducted has revealed that:

- the formation of interparticle contacts, i.e. microstructural development, does affect the rate of hydration of individual particles substantially. *Hydration and microstructural development should, therefore, be considered (and modelled) as mutually interrelated phenomena.* Ignoring microstructural development as a factor in hydration kinetics may give rise to misinterpretations as regards interpreting the results of experimental hydration data.
- the particle size distribution of the cement is an important factor in both hydration kinetics and microstructural development (see also [2]).
- the amount of cement which is involved in the development of interparticle contacts and which is a measure of the number of interparticle contacts, appears to exhibit a good correlation with strength development. As also shown by experiments particle fractions play a major role in the formation of interparticle contacts and in the development of strength (2).
- having modelled the effects of the *particle size distribution*, the *w/c ratio* and the *reaction temperature* on the rate of hydration, the effect of the chemical composition of (Portland) cement was described with *two* model parameters, i.e., the basic rate factor $K_0(C_3S)$, which could be written as a function of the C_3S content, and the transition thickness $\delta_{tr}(C_2S)$, which

appeared to be weakly correlated to the C_2S content.
the majority of isothermal and adiabatic hydration data analyzed so far has revealed that the hydration of Portland cement-based systems could be predicted with an accuracy at 28 days between ten and fifteen percent. Higher accuracies are not expected to be possible unless the effects of C_3A, the gypsum content and minor constituents are also considered in the model.

Although promising results have been obtained, it is emphasized that the model is still in its early stage of development. Further research is planned as regards the difference between paste hydration and hydration in actual concretes, modelling of hydration of non-Portland cements, the effect of additives and extra fines and pore water chemistry.

References

1. I. Odler, Th. von Borstel, Cem. Concr. Res. 19, 295 (1989).
2. K. van Breugel, Simulation of hydration and formation of structure in hardening cement-based materials, p. 295, W.D. Meinema, Delft, 1991.
3. F.H. Wittmann, 7th Int. Congr. Chem. Cem., Paris, Vol. I, pp. VI-2 / 1-14 (1980).
4. W. Lerch, C.L. Ford, Journ. Am. Concr. Inst., 44, 745 (1948).
5. K. Scrivener, A. Bentur, P.L. Pratt, Adv. Cem. Res., I, 230 (1988).
6. S. Diamond, Mat. Res. Soc., Proc. 85, 21 (1986).
7. U. Danielsson, 4th. Int. Symp. Chem. Cem., Washington, I, 519 (1960).
8. Dutch Cement Industry, Privately received documentation on adiabatic tests.
9. K. van Breugel, "Numerical simulation of hydration and microstructural development in hardening cement-based materials - Part I - Theory," Cem. Concr. Res., 25, 319-331, 1995.
10. T.C., Powers, *Ibid. [20].*
11. G. Fagerlund, Seminar on Hydration of Cement, Copenhagen, p. 56, (1987).
12. F.O. Anderegg, D.S. Hubbell, Proc. Am. Soc. Test. Mat., 29, (1929).
13. G. Krogbeumker, U. Ludwig, Zement-Kalk-Gips, 25, 417 (1972).
14. A.R. Steinherz, A.R., Rev. Mat. Constr. Trav. Publ., 536, (1960).
15. S. Tsumura, Zement-Kalk-Gips, 19, 511 (1966).
16. P. Lhopitallier, L.M. James, XXI Congr. Chem. Ind., Bruxelles, (1948).
17. J.H. Taplin, 5th Int. Congr. Chem. Cem., Tokyo, paper II-70, 337 (1968).
18. A. Bezjak, I. Jelenic, V. Mlakar, A. Panovic, 7th Int. Congr. Chem. Cem., Paris, II, 111 (1980).
19. M. Venaut, Rev. Mat. & Constr., 549, 333, 552, 393 (1961).
20. F.W. Locher, Beton, H. 7, 247, H. 8, 283 (1976).
21. K. Rakel, Beitrag zur Bestimmung der Hydratationswärme von Zement, PhD, Aachen, p. 149, 1965).
22. K.O. Kjellsen, R.J. Detwiler, O.E. Gjørv, Cem. Concr. Res., 21, 179 (1991).
23. E.A.B. Koenders, K. van Breugel, Thermal cracking in Concrete at Early Ages, Ed. R. Springenschmid, E. & F. Spon, London, 3 (1994).
24. K. van Breugel, Thermal cracking in Concrete at Early Ages, Ed. R. Springenschmid, E. & F. Spon, London, 127 (1994).